

# UNCLASSIFIED

<b>AD NUMBER</b>
ADB241898
<b>NEW LIMITATION CHANGE</b>
<b>TO</b> Approved for public release, distribution unlimited
<b>FROM</b> Distribution authorized to U.S. Gov't. agencies only; Proprietary Info.; Aug 98. Other requests shall be referred to US Army Medical Research and Materiel Comd., Fort Detrick, MD 21702-5012.
<b>AUTHORITY</b>
USAMRMC ltr dtd 26 Jan 2000

THIS PAGE IS UNCLASSIFIED

AD \_\_\_\_\_

GRANT NUMBER DAMD17-94-J-4080

TITLE: Topology and Function of Human p-Glycoprotein in  
Multidrug Resistant Breast Cancer Cells

PRINCIPAL INVESTIGATOR: Ernest S. Han  
Luis Reuss, M.D.

CONTRACTING ORGANIZATION: University of Texas Medical Branch  
Galveston, Texas 77555

REPORT DATE: August 1998

TYPE OF REPORT: Final

PREPARED FOR: Commander  
U.S. Army Medical Research and Materiel Command  
Fort Detrick, Frederick, Maryland 21702-5012

DISTRIBUTION STATEMENT: Distribution authorized to U.S. Government agencies only (proprietary information, Aug 98). Other requests for this document shall be referred to U.S. Army Medical Research and Materiel Command, 504 Scott Street, Fort Detrick, Maryland 21702-5012.

The views, opinions and/or findings contained in this report are those of the author(s) and should not be construed as an official Department of the Army position, policy or decision unless so designated by other documentation.

DTIC QUALITY INSPECTED 2

## NOTICE

USING GOVERNMENT DRAWINGS, SPECIFICATIONS, OR OTHER DATA INCLUDED IN THIS DOCUMENT FOR ANY PURPOSE OTHER THAN GOVERNMENT PROCUREMENT DOES NOT IN ANY WAY OBLIGATE THE U.S. GOVERNMENT. THE FACT THAT THE GOVERNMENT FORMULATED OR SUPPLIED THE DRAWINGS, SPECIFICATIONS, OR OTHER DATA DOES NOT LICENSE THE HOLDER OR ANY OTHER PERSON OR CORPORATION; OR CONVEY ANY RIGHTS OR PERMISSION TO MANUFACTURE, USE, OR SELL ANY PATENTED INVENTION THAT MAY RELATE TO THEM.

### LIMITED RIGHTS LEGEND

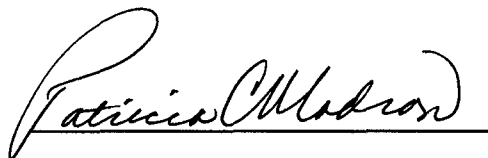
Award Number: DAMD17-94-J-4080

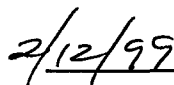
Contractor: University of Texas Medical Branch

Location of Limited Rights Data (Pages): 12-25

Those portions of the technical data contained in this report marked as limited rights data shall not, without the written permission of the above contractor, be (a) released or disclosed outside the government, (b) used by the Government for manufacture or, in the case of computer software documentation, for preparing the same or similar computer software, or (c) used by a party other than the Government, except that the Government may release or disclose technical data to persons outside the Government, or permit the use of technical data by such persons, if (i) such release, disclosure, or use is necessary for emergency repair or overhaul or (ii) is a release or disclosure of technical data (other than detailed manufacturing or process data) to, or use of such data by, a foreign government that is in the interest of the Government and is required for evaluational or informational purposes, provided in either case that such release, disclosure or use is made subject to a prohibition that the person to whom the data is released or disclosed may not further use, release or disclose such data, and the contractor or subcontractor or subcontractor asserting the restriction is notified of such release, disclosure or use. This legend, together with the indications of the portions of this data which are subject to such limitations, shall be included on any reproduction hereof which includes any part of the portions subject to such limitations.

THIS TECHNICAL REPORT HAS BEEN REVIEWED AND IS APPROVED FOR PUBLICATION.

  
\_\_\_\_\_

  
\_\_\_\_\_

REPORT DOCUMENTATION PAGE			Form Approved OMB No. 0704-0188	
Public reporting burden for this collection of information is estimated to average 1 hour per response, including the time for reviewing instructions, searching existing data sources, gathering and maintaining the data needed, and completing and reviewing the collection of information. Send comments regarding this burden estimate or any other aspect of this collection of information, including suggestions for reducing this burden, to Washington Headquarters Services, Directorate for Information Operations and Reports, 1215 Jefferson Davis Highway, Suite 1204, Arlington, VA 22202-4302, and to the Office of Management and Budget, Paperwork Reduction Project (0704-0188), Washington, DC 20503.				
1. AGENCY USE ONLY (Leave blank)		2. REPORT DATE August 1998	3. REPORT TYPE AND DATES COVERED Final (1 Sep 94 - 31 Aug 98)	
4. TITLE AND SUBTITLE Topology and Function of Human p-Glycoprotein in Multidrug Resistant Breast Cancer Cells			5. FUNDING NUMBERS DAMD17-94-J-4080	
6. AUTHOR(S) Mr. Ernest S. Han				
7. PERFORMING ORGANIZATION NAME(S) AND ADDRESS(ES) University of Texas Medical Branch Galveston, Texas 77555-0641			8. PERFORMING ORGANIZATION REPORT NUMBER	
9. SPONSORING / MONITORING AGENCY NAME(S) AND ADDRESS(ES) U.S. Army Medical Research and Materiel Command Fort Detrick, Maryland 21702-5012			10. SPONSORING / MONITORING AGENCY REPORT NUMBER	
11. SUPPLEMENTARY NOTES  <div style="text-align: center; font-size: 2em; font-weight: bold;">19990225195</div>				
12a. DISTRIBUTION / AVAILABILITY STATEMENT Distribution authorized to U.S. Government agencies only (proprietary information, Aug 98). Other requests for this document shall be referred to U.S. Army Medical Research and Materiel Command, 504 Scott Street, Fort Detrick, Maryland 21702-5012.			12b. DISTRIBUTION CODE	
13. ABSTRACT (Maximum 200 words) Overexpression of P-glycoprotein (Pgp) in breast and other cancers is thought to be largely involved in the development of multidrug resistance to chemotherapy. Pgp has been reported to have multiple topologies and multiple functions. The goal of our research is to investigate the relationship between Pgp structure and its multiple functions. Here, we examined in detail the topologies of the C-terminal half of Pgp. We found that transmembrane (TM) 8 may be important in the generation of multiple topological orientations. In addition, when TM8 initiated membrane insertion, TM9 was found to stop the translocation event and anchor into the membrane. Based on our findings, a model for the C-half topology is proposed. Previously, we were able to manipulate the generation of C-half topologies by altering the charge distribution flanking TM8. Here, we transfected Pgp constructs that contained these alterations in charge distribution into the mouse fibroblast cell line, BALB/c-3T3. Expression of Pgp was determined by quantitative western blot analysis and both drug transport and regulation of swelling-activated chloride currents were examined. To date our results are incomplete to draw any conclusions about the relationship between Pgp topology and function. An update of our progress is discussed.				
14. SUBJECT TERMS Breast Cancer			15. NUMBER OF PAGES 32	
			16. PRICE CODE	
17. SECURITY CLASSIFICATION OF REPORT Unclassified		18. SECURITY CLASSIFICATION OF THIS PAGE Unclassified		19. SECURITY CLASSIFICATION OF ABSTRACT Unclassified
				20. LIMITATION OF ABSTRACT Limited

## FOREWORD

Opinions, interpretations, conclusions and recommendations are those of the author and are not necessarily endorsed by the U.S. Army.

\_\_\_\_ Where copyrighted material is quoted, permission has been obtained to use such material.

\_\_\_\_ Where material from documents designated for limited distribution is quoted, permission has been obtained to use the material.

EH Citations of commercial organizations and trade names in this report do not constitute an official Department of Army endorsement or approval of the products or services of these organizations.

EH In conducting research using animals, the investigator(s) adhered to the "Guide for the Care and Use of Laboratory Animals," prepared by the Committee on Care and use of Laboratory Animals of the Institute of Laboratory Resources, national Research Council (NIH Publication No. 86-23, Revised 1985).

\_\_\_\_ For the protection of human subjects, the investigator(s) adhered to policies of applicable Federal Law 45 CFR 46.

EH In conducting research utilizing recombinant DNA technology, the investigator(s) adhered to current guidelines promulgated by the National Institutes of Health.

EH In the conduct of research utilizing recombinant DNA, the investigator(s) adhered to the NIH Guidelines for Research Involving Recombinant DNA Molecules.

EH In the conduct of research involving hazardous organisms, the investigator(s) adhered to the CDC-NIH Guide for Biosafety in Microbiological and Biomedical Laboratories.

PI - Signature

9/10/98

Date

## TABLE OF CONTENTS

PAGE	
1	Front Cover
2	SF 298 Documentation
3	Foreword
4	Table of Contents
5	Introduction
	Body of Final Report
7	Methods
11	Results/Discussion
26	Conclusions
28	References
30	Appendix

## INTRODUCTION

### BACKGROUND AND SIGNIFICANCE

Chemotherapy often fails because breast and other cancers become resistant or are intrinsically resistant to various unrelated chemotherapeutic agents. This phenomenon has been described as multidrug resistance or MDR (1;2). The overexpression of P-glycoprotein (Pgp) is thought to be largely involved in causing MDR. However, our understanding of how Pgp confers MDR is incomplete. The focus of this research is to examine the relationship between Pgp structure and function to gain insight into the mechanisms involved in chemotherapy failure for the treatment of breast cancer and other malignancies.

#### I. Structure of P-glycoprotein

P-Glycoprotein is a member of a large group of transporters known as the ABC (or ATP-binding cassette) superfamily which also includes other important proteins such as the cystic fibrosis transmembrane conductance regulator (CFTR) (1;2). This superfamily is generally characterized by a structural motif, which contains two homologous halves, each consisting of six putative transmembrane (TM) segments followed by a nucleotide-binding domain. However, the membrane folding of Pgp TM segments is more complex than previously thought. Both a hydropathy-predicted topology (3-5) and alternative topologies (6-11) have been observed for Pgp. Because more than one topological orientation has been observed, an interesting question arises as to what mechanisms are involved in generating these topologies.

Our previous studies have focused in part on understanding the molecular mechanism for the multiple foldings of the carboxyl-terminal half (C-half) of Pgp. We made the observation that the cytoplasmic-predicted loop between TM8 and TM9 was glycosylated, suggesting that the C-half of Pgp has a topology not predicted from the hydropathy model (see Annual Report 1994-1995). In addition, our results suggested that TM8 may possess unique membrane insertion properties. We found that TM8 in the presence of TM7 may function as a signal sequence to initiate membrane insertion with its amino- and carboxyl- terminal ends located in the cytoplasmic and exoplasmic spaces, respectively (see Annual Report 1996-1997 and ref.6). In addition, TM8 was found to possess stop-transfer activity (i.e. stops the translocation event across the membrane) when preceded by the strong signal-anchor sequence TM1 (see Annual Report 1996-1997). This stop-transfer activity of TM8 is consistent with the hydropathy-predicted model for C-half Pgp (6). Although these observations suggest that the membrane folding of TM8 is complex, the individual membrane insertion property of both TM7 and TM8 is currently not known. In addition, an important issue is raised regarding the consequences of TM8 membrane insertion properties on the topological folding of downstream TM segments (e.g., TM9 and TM10). Previously, Zhang *et al.* examined the membrane insertion of TM11 and TM12 from Chinese hamster *pgp1* Pgp and found that the

membrane insertion of TM11 and TM12 was consistent with the hydropathy-predicted model (12). However, it is still not understood how TM9 and TM10 of Pgp insert and fold in the membrane when TM8 functions as a signal sequence to initiate insertion into the membrane.

## **II. Function of P-glycoprotein**

Numerous studies have shown that Pgp actively transports a diverse group of substrates out of cells (15;16). In addition to its transport function, Pgp has been reported to express a second function. Evidence is now accumulating in support of Pgp functioning as a Cl<sup>-</sup> channel regulator (17-19). Initially, Pgp expression was found to be associated with swelling-activated Cl<sup>-</sup> currents ( $I_{Cl,swell}$ ) (20;21). However in an attempt to confirm these initial findings, several groups found that  $I_{Cl,swell}$  was independent of Pgp expression (17;22-24). Recently, two experimental findings strongly support a relationship between Pgp and  $I_{Cl,swell}$ . First,  $I_{Cl,swell}$  was shown to be regulated by PKC phosphorylation of Pgp (18). Second, we and others have demonstrated that the  $I_{Cl,swell}$  can be inhibited by the anti-Pgp monoclonal antibody C219 in Pgp-expressing cells (17;19;25); see also Annual Report 1994-1995). In addition, Vanoye *et al.* (19) have found through detailed electrophysiological experiments that Pgp is not a swelling-activated Cl<sup>-</sup> channel, but likely a Cl<sup>-</sup> channel regulator. In support of the notion that Pgp can regulate endogenous channels, other members of the ABC superfamily of transporters (e.g., CFTR) have also been observed to regulate endogenous channels (26;27).

Since Pgp has been observed to support two distinct functions, one of the main goals of this research was to investigate if the two functions of Pgp were correlated with the observed topologies. Previously, we reported that certain Pgp topologies could be predominantly expressed in a cell-free system by altering the charge distribution flanking TM8 (see Annual Report 1996-1997 and ref.6). Increasing the net positive charge C-terminal to TM8 favored a hydropathy-predicted model. However, generation of an alternative topology was facilitated when the C-terminal region flanking TM8 had less net positive charge. This suggested that the C-half topology could be manipulated. Here, we undertook the study to express full-length Pgp molecules containing these charge mutations in a mouse fibroblast cell line and then assessed Pgp functions.



## BODY OF FINAL REPORT

### METHODS

#### I. Generation of Pgp cDNA Constructs

For studies involving the membrane folding of C-half Pgp TM segments, several truncated Pgp constructs were created. In all Pgp truncated molecules generated, it is noteworthy that the flanking 15 amino acids of TM segments were retained in order to preserve the topogenic information necessary to direct TM orientation (28). To generate TM8R, we performed recombination PCR. Briefly, a region encoding a translation initiation sequence was amplified using TM1/8R template (see Annual Report 1996-1997 and ref.6), universal primer SP6, and a chimeric primer (5'TTCATCA-TCAGTATTCTCCATCACG-3'). Then, a second PCR reaction was performed using the amplified cassette, universal primer T7, and TM1/8R template. The final PCR product was ligated into the Hinc II site of pGEM-4z vector (Promega). TM8R encodes TM8 with its flanking sequences (Asn<sup>739</sup>-Met<sup>788</sup>) followed by a glycosylation reporter molecule (7).

TM7R was generated with a one-step PCR reaction using the following template and primers: pGHaPGP-C6 template (see Annual Report 1994-1995 and (6)), primer A693a (5'-GTCGTGATGGAGTCCTTTTGGCGT-3'), and primer B746a (5'-CAAGATCTGTCGTTTGGTTTC-3'). The PCR product was digested with Bgl II and ligated to a pGEM-4z vector along with the reporter sequence (plasmid pGPGP-N3 (7) digested with Bgl II and Hind III). TM7R encodes the amino acids from Ser<sup>693</sup>-Arg<sup>746</sup> followed by a reporter molecule.

To create TM8-9R construct, we replaced the TM5-encoding regions of TM5R (J.T.-Zhang, E.Han, and C.Wang, submitted) with two DNA fragments, which together encode TM8 and TM9 with their flanking sequences. We used the following DNA fragments: (1) EcoR I-Sty I fragment (encodes N-terminal flanking sequence of TM8 and part of TM8) from TM8R (6) and (2) a Sty I- Hinc II fragment (encodes TM9 and part of TM8) from a Pgp cDNA that contains only TM8 to TM12. These two fragments were ligated into TM5R construct that was digested with Bgl II, treated with Klenow, and then followed by EcoR I digestion. TM8-9R construct encodes Asn<sup>739</sup> to Gln<sup>853</sup> of Pgp, two additional amino acids (Met and Glu) at the amino-terminal end for translation initiation and a glycosylation reporter at the carboxyl-terminal end.

TM7-9R construct was generated by performing a three-fragment ligation. These fragments included (1) a Sac I-Mse I fragment (encodes TM7 and TM8) which was derived from pGHaPGP-C6 DNA (6), (2) a Mse I-Hind III fragment (encodes TM9 and a glycosylation reporter molecule) which was derived from TM9R (J.T.-Zhang, E.Han, and C.Wang, submitted), and (3) pGEM-4z vector linearized with Sac I and Hind III. TM7-9R construct encodes TM segments 7 to 9 (Met<sup>613</sup>-Gln<sup>853</sup>) followed by a glycosylation reporter.

Three-fragment DNA ligation was also used to create TM7-10R construct with the following fragments: (1) Sac I-Ava I (Ava I site was treated with Klenow) fragment (encodes TM7 through TM10) which was derived from pGHaPGP-C6 (6), (2) SspI-Hind

III fragment (encodes the glycosylation reporter) which was derived from pGPGP-N3R (7), and (3) pGEM-4z vector linearized with Sac I and Hind III. TM7-10R construct contains TM segments 7 through 10 (Met<sup>613</sup>-Leu<sup>907</sup>) followed by a glycosylation reporter.

For experiments involving the addition of consensus sites for N-linked glycosylation within TM9, we performed recombination PCR (6). Using a Pgp construct that contains the complete C-half TM domain (pGHaPGP-C6; see Annual Report 1994-1995 and (6)), we replaced Gly<sup>841</sup> with a serine residue to create NG-1. NG-2 contained mutations of Ala<sup>838</sup> and Gly<sup>841</sup> to serine residues. For the first PCR reaction, the following primers and template were used: primer NG-1p (5'-AGCAAATCTGTCGACAAGA-3') for NG-1 or primer A2611 (5'-ATATC-AAATCTGTCGACAGGAAT-3') for NG-2, universal primer T7, and DNA template pGHaPGP-C6 (6). The second PCR reaction included the first PCR product, the universal primer SP6 and template pGHaPGP-C6. For NG-1, the final PCR product was digested with Sac I and Xba I and ligated to a fresh pGEM-4z vector digested with the same restriction enzymes. For NG-2, the final PCR product was digested with Bsm I and Mfe I and ligated to pGHaPGP-C6 DNA digested with the same restriction enzymes. We performed DNA sequencing to confirm that no errors were introduced during the generation of all Pgp constructs.

## **II. *In vitro* Transcription and Translation Using a Cell-Free System**

To generate run-off transcripts, wild-type and mutant cDNA templates were linearized with a restriction enzyme and transcribed with either SP6 or T7 RNA polymerase in the presence of a cap analog m<sup>7</sup>G(5')ppp(5')G. After transcription, the DNA template was removed by RQ1 DNase and RNA transcripts were purified by standard methods.

The run-off transcripts were used to direct translation of proteins using the rabbit reticulocyte lysate (RRL) translation system in the presence of dog pancreatic microsomal membranes (RM), as suggested by the supplier (Promega). High speed centrifugation (13,200 rpm, 4°C) was performed on translation products to separate membrane (pellet) and non-membrane (supernatant) associated fractions. The pellet fraction was isolated and resuspended in STBS solution (in mM: 250 sucrose, 10 Tris-HCl, pH 7.5, 150 NaCl) for further processing. For experiments requiring protease digestion and endoglycosidase treatment of membrane fractions, samples were exposed to 0.2 mg/ml proteinase K for 20 min at room temperature. After addition of PMSF (10 mM final concentration) to stop the reaction, the translation material was pelleted and washed with STBS solution containing PMSF. The pellet was resuspended in a reaction mix containing the following: (in mM) 50 sodium phosphate buffer (pH 7.6), 1.25% NP-40, 0.5% 2-mercaptoethanol, 2 PMSF, 1 unit PNGase F (or equivalent volume of water for control samples), and 0.2% SDS. After incubation for at least 1 hr, electrophoresis buffer was added and the sample was analyzed by SDS-PAGE and fluorography.

## **III. Transfection of Pgp Constructs**

Generation of Pgp constructs which contained mutations that alter TM topology *in vitro*, were previously described in the Methods section from Annual Report 1996-1997.

Essentially, full-length Pgp cDNA (wild-type or containing charge mutation) was inserted into the expression vector, pLK444M (29). Insertion of the Pgp sequence was adjacent to a  $\beta$ -actin promoter, which directs its expression. Also, the expression vector contains a neomycin phosphotransferase gene, which confers resistance to the antibiotic neomycin (G418). The mouse fibroblast cell line, BALB/c-3T3 cells, was transfected with either full-length Pgp cDNA or the vector alone (pLK444M) using lipofectamine (Gibco BRL). Essentially, cells were plated in a 100x20mm tissue culture dish to 30-40% confluency in Dulbecco's modified Eagle's medium (DMEM) supplemented with 10% fetal bovine serum (Gibco BRL) and 1% (v/v) penicillin-streptomycin (P-S; 1 unit penicillin, 1  $\mu$ g streptomycin; Gibco BRL). Cells were washed twice in medium without FBS and P-S and incubated in the same medium containing a lipofectamine-DNA mixture (10  $\mu$ g lipofectamine- 10  $\mu$ g DNA) in a 37°C incubator (5%CO<sub>2</sub>) for 6 hrs. Then, FBS (10% final) and P-S (1% final) were added, and 48 hrs later, G418 (600  $\mu$ g/ml final concentration) was added to select for cells transfected with Pgp or vector DNA. Approximately 2 weeks later, G418-resistant colonies were isolated by cloning cylinders and propagated for subsequent studies.

#### **IV. Determination of Pgp Expression in Cells**

To determine quantitatively the expression of Pgp in the various colonies isolated, we first attempted to use flow cytometry to assess cell surface expression by indirect immunofluorescence staining with commercially available anti-Pgp antibodies (264/F4 and F4 (Kamiya)). These antibodies were selected based on their reported cross-reactivity to hamster Pgp. However, we were unsuccessful in obtaining any significant labeling above background using these antibodies. Therefore, we took an alternative approach to assess Pgp expression.

We used quantitative Western Blot analysis to examine expression of Pgp. To prepare membranes, cells were harvested from 145x20 mm tissue-culture dishes by scraping and washed twice in phosphate-buffered saline solution (PBS, pH 7.4). Then, cells were incubated in hypotonic lysis buffer (in mM: 10 KCl, 1.5 MgCl<sub>2</sub>, 10 Tris/HCl, pH 7.4, 0.1 phenylmethylsulfonyl fluoride (PMSF)) on ice for 1hr with continuous shaking. Unbroken cells were separated from lysed cells by isolating the pellet fraction after centrifugation (2500 rpm), while the supernate was kept on ice. The pellet was resuspended in hypotonic-lysis buffer, further disrupted by a dounce homogenizer ( $\approx$  40 strokes), and centrifuged (5700 rpm, 4°C). The homogenization procedure was repeated and the supernate fractions were pooled. The supernate was then centrifuged in an ultracentrifuge (SW28 rotor, Beckman) at 23,000 rpm for 1 hr at 4°C. The supernate was removed and the pellet was resuspended in STBS buffer containing 100  $\mu$ M PMSF. Protein concentration was measured by the Bicinchoninic Acid (BCA) assay (Pierce), and 150  $\mu$ g of membrane protein was subjected to SDS-PAGE. Upon completion, proteins were transferred to PVDF membranes (Bio-Rad) by electroblotting. PVDF membranes were then probed with monoclonal anti-Pgp antibody, C494, followed by horseradish-peroxidase-conjugated secondary antibody. After treating PVDF membranes with

SuperSignal Ultra Chemiluminescence kit (Pierce), signals were detected on film and quantified using densitometry (Lynx Software, v. 5.5).

Serial dilutions of membranes isolated from the multidrug-resistant CH<sup>R</sup>B30 cells were included in each gel to ensure that the chemiluminescence signal was not saturating. Densitometric readings from the serially diluted CH<sup>R</sup>B30 membranes were plotted against the amount of membranes analyzed, and a polynomial fit was generated. Then, the equivalent amount of CH<sup>R</sup>B30 membranes was estimated from the densitometric readings of the Pgp constructs examined. Most Pgp constructs analyzed were within the linear range of chemiluminescence signal detection (see RESULTS/DISCUSSION).

## **V. Unidirectional Efflux of Rhodamine 123**

To examine the drug transport function of Pgp, we determined the unidirectional efflux of the fluorescent Pgp substrate, rhodamine 123 (R123) (30). Essentially, cells were plated on a glass coverslip overnight to near confluency. Then, cells were loaded for 1 h at room temperature with 10  $\mu$ M R123 in a Hepes-buffered solution (HBS; in mM: 135 NaCl, 5 KCl, 1 MgCl<sub>2</sub>, 2 CaCl<sub>2</sub>, 7.8 glucose, 5 Hepes; titrated to pH 7.4 with NaOH) containing 5  $\mu$ M verapamil. After R123 loading, the coverslip was mounted in a Leiden microincubator (Medical Systems) on the stage of an inverted microscope and constantly superfused with R123-free HBS. The decrease in intracellular R123 fluorescence ( $F_{R123}$ ) was continuously measured for a population of 50-100 cells. The decay in  $F_{R123}$  follows a single exponential (30), and a rate constant ( $k$ ) was estimated by fitting the data to the following equation:

$$F_{R123} = F_o + F_{R123}(0)\exp(-kt),$$

where  $F_o$  is the background fluorescence,  $F_{R123}(0)$  is  $F_{R123}$  at time ( $t$ ) = 0

## **VI. Flow Cytometric Analysis of Pgp Mutant Clones**

For experiments testing whether flow cytometry could be used to distinguish different cell populations expressing Pgp, cells were grown in T25 culture flasks to near confluency and loaded with 10  $\mu$ M R123 in culture medium to steady-state (37°C incubator with 5% CO<sub>2</sub>; 1 h). The medium was then replaced with R123-free medium. After incubating the cells for different times (see Figure 11) at room temperature, the cells were treated with trypsin to detach the cells from the flask, washed with phosphate-buffered saline (PBS, pH 7.4), resuspended in PBS to a cell-density of  $\approx 2 \times 10^6$  cells/ml, and kept on ice for the remaining period.

Flow cytometric analysis was performed using the FACS Vantage cell sorter (Becton-Dickinson). Cells were excited at 488 nm wavelength and analyzed with a band pass filter of 525 nm. 9000-1050 events were captured. Data were analyzed using Windows Multiple Document Interface (WinMDI) Flow Cytometry Application software (v.2.7; by Joseph Trotter).

## RESULTS/DISCUSSION

### I. Topological Analysis of C-Terminal Half Pgp

Initially, we proposed to study the topology of Pgp expressed in breast cancer cells (see Statement of Work from original Research Proposal). However, we have utilized an *in vitro* system for the topological analysis of Pgp instead of an intact cell system for several reasons (see also previous Annual Report 1996-1997). This cell-free system is very convenient and has allowed us to rapidly assess the membrane topology of Pgp. We have continued to use this approach since we have been able to examine the detailed mechanism of generating C-half Pgp topology. Here, we investigated the detailed membrane folding of C-half Pgp, specifically TM7 through TM10. In addition, we examined the mechanism of regulation by ribosomes on determining the TM topology of C-half Pgp.

#### I.1 *Membrane Insertion Activity of TM8 in the Topogenesis of C-Half Pgp.*

Previously using TM7-8R construct, we found that TM8 re-initiated insertion into the membrane suggesting that TM8 has signal-anchor activity. To examine more directly the signal-anchor activity and membrane orientation of TM8, we created a truncated Pgp construct that contains TM8 followed by a glycosylation reporter (TM8R; Fig. 1A). Translation of TM8R in RRL resulted in a 35-kDa product (Fig. 1B, lane 1). It is noteworthy that translation of TM7-8R RNA resulted in a higher molecular weight translation product (50 kDa) as expected (Fig. 1, lane 4). In the presence of RM, a majority of TM8R products shifted to 38 kDa and were membrane-associated (Fig. 1B, lane 2). This 38-kDa band was sensitive to PNGase F treatment (Fig. 1B, lane 3) and resistant to proteinase K digestion (Fig. 1C, lanes 1-2). These results suggest that the large reporter domain ( $\approx 32$  kDa) of TM8R was translocated into the RM lumen and glycosylated (see Fig. 1E, model II). The observation of a similar 38-kDa peptide after proteinase K treatment of membranes containing TM7-8R (Fig. 1, lanes 4-5) corroborate the notion that TM8 and the reporter sequence are protected by the membrane from protease digestion. Thus, TM8 alone contains a signal-anchor activity and inserts into membranes predominantly in a  $N_{\text{cyt}}-C_{\text{exo}}$  orientation.

Since our previous results suggested that TM8 in the presence of TM7 can function as a signal-anchor sequence, TM7 may fold into membranes as two TM segments as proposed by Béjà & Bibi (ref.11; see Fig.1E, model V). Therefore, we examined the membrane insertion properties of TM7 by creating a construct containing TM7 followed by a glycosylation reporter (TM7R; Fig. 1A). Translation in the absence or presence of RM both resulted in a 35-kDa product (Fig. 1D, lanes 1-2) suggesting that no glycosylation occurred in the presence of RM. When we tested the membrane integration properties of TM7R product, we found that the 35-kDa product was not associated with the membrane fraction after centrifugation (Fig. 1D, lanes 3-4). These results suggest that TM7 alone cannot insert into membranes (Fig. 1E, model VI). Therefore, TM7 likely does not have *de novo* membrane insertion activities.

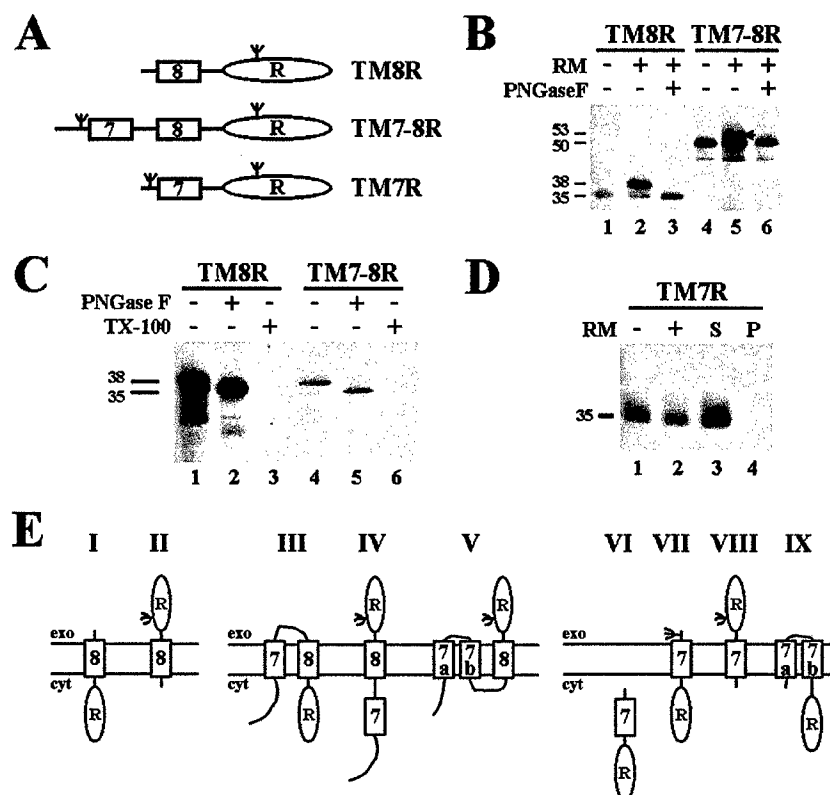
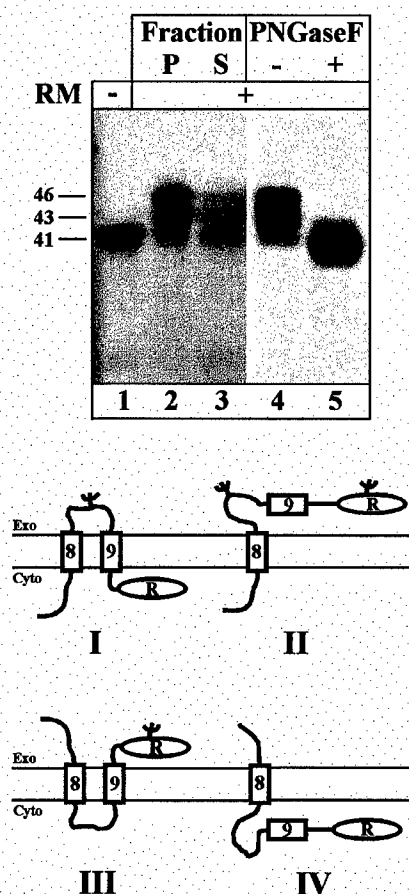


**Figure 1. Membrane insertion and topology of TM7 and TM8.** (A) Schematic diagram of the Pgp constructs, TM8R, TM7-8R, and TM7R. Putative TM segments are shown as rectangular boxes and the glycosylation reporter molecule is indicated as an oval. Branched symbols denote consensus sites for N-linked glycosylation. (B) Analysis of N-linked glycosylation for TM8R and TM7-8R. Lanes 1 and 4 represent translation products in the absence of RM. Lanes 2 and 5 and lanes 3 and 6 show membrane-associated products without or with PNGase F treatment, respectively. (C) Proteinase K treatment of RM containing TM8R or TM7-8R translation products. Proteinase K digestion was performed in the absence (lanes 1 and 4) or presence of Triton X-100 (lanes 3 and 6). Membrane-protected fragments were further treated with PNGase F (lanes 2 and 5). (D) Membrane insertion of putative TM7. Translation of TM7R in RRL was performed in the absence (lane 1) or presence (lane 2) of RM. Supernate and pellet fractions were separated after centrifugation (lanes 3-4). (E) Topological models for TM8R (models I and II), TM7-8R (models III-V), and TM7R (models VI-IX).

## I.2 Membrane Topology of TM8-9R Construct.

We found that TM8 can initiate membrane insertion in a  $N_{\text{cyt}}\text{-}C_{\text{exo}}$  orientation, and TM11 and TM12 have been previously observed to insert into the membranes as predicted (12). Taken together, these findings suggest that the membrane folding of TM9 and TM10 is complex. Specifically, it was not clear whether TM9 or TM10 functions as a stop-transfer sequence to anchor into the membrane. To address this issue, we generated a DNA construct that codes for a protein sequence which contains putative TM segments 8 and 9 followed by a glycosylation reporter sequence (named TM8-9R; see METHODS, sec. I). Figure 2 shows that translation of TM8-9R transcript in the rabbit reticulocyte lysate system in the absence of microsomal membranes (RM) resulted in a 41-kDa product (lane 1). In the presence of RM, two major products of 46 and 43 kDa were observed (Fig. 2, lane 2). Both products were associated with the membrane pellet fraction after centrifugation, indicating that the translation products were membrane associated (Fig. 2, compare lanes 2 and 3). Endoglycosidase PNGase F treatment shifted both the 46- and 43-kDa products to 41 kDa (Fig. 2, lanes 4 and 5). Thus, both the 46- and 43-kDa products were glycosylated and inserted into membranes. The size difference between glycosylated and deglycosylated products suggests that 1 and 2 N-linked sugars

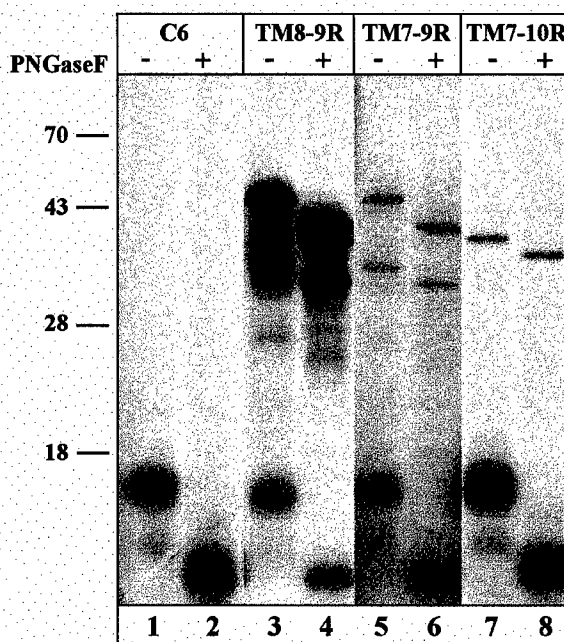
**Figure 2. Translation of TM8-9R construct.** TM8-9R transcript was translated in the absence (lane 1) or presence of RM (lanes 2-5). Translation products were centrifuged to separate membrane (lane 2) and non-membrane fractions (lane 3). Membrane fractions were further treated with control solution (lane 4) or PNGase F (lane 5). Models of TM8-9R topology are shown below. Rectangular boxes, oval symbols, and branched symbols represent TM segments, reporter molecule and N-linked sugars, respectively.



were attached to the 43- and 46-kDa products, respectively, assuming the high mannose core sugar that was added has a molecular size of approximately 2.5 kDa. It should be noted that the consensus sequences for N-linked glycosylation in TM8-9R construct are located in the loop between TM8 and TM9 and also within the reporter sequence. Based on our results, several topological orientations for TM8-9R are possible (Fig. 2). A potential topology for the 46-kDa product is represented by model II (Fig. 2) where both consensus sites for N-linked glycosylation were used. For the 43-kDa product, which contains only one sugar, either glycosylation site could be used and their predicted topologies are depicted in models I and III (Fig. 2). It is noteworthy that a minor 41-kDa product was observed in the membrane fraction (Fig. 2, lane 2). This unglycosylated product is consistent with model IV topology, which lacks N-linked sugars.

To test these models of TM8-9R topology, we treated membrane-associated TM8-9R products with proteinase K, which digests accessible regions exposed to the cytoplasmic space (i.e., outside of the membrane vesicles). After proteinase K treatment,

**Figure 3. Membrane-protected fragments from various Pgp constructs after proteinase K treatment.** Isolated membranes containing translation products were treated with proteinase K alone (lanes 1, 3, 5, and 7) or proteinase K followed by PNGase F treatment (lanes 2, 4, 6, and 8).



we observed both 17- and 45-kDa peptides as well as other bands which are discussed below (Fig. 3, lane 3). Both the 17- and 45-kDa protected fragments were glycosylated since these bands shifted to 14 and 40 kDa after PNGase F treatment, respectively (Fig. 3, lane 4). This suggests that the 45-kDa product contains two N-linked sugars, while the 17-kDa product has only one sugar attached. The observation of a 45-kDa membrane-protected peptide that contains 2 sugars indicates that both the loop between TM8 and TM9 and also the reporter molecule are located within the ER lumen. Based on model II (Fig. 2), proteinase K is predicted to have access only to the amino-terminal flanking sequences of TM8, and thus a small change in molecular size would be expected ( $\approx 2$  kDa). Our observation of a change from 46- to 45-kDa after proteinase K treatment is consistent with model II topology. Interestingly, the 17-kDa peptide derived from TM8-



kDa). Our observation of a change from 46- to 45-kDa after proteinase K treatment is consistent with model II topology. Interestingly, the 17-kDa peptide derived from TM8-9R had the same mobility as the membrane-protected product that resulted from treatment of membranes containing the complete C-half TM domain (Fig. 3, compare lanes 1 and 3). We have previously shown that this 17-kDa protein fragment was immunoreactive to an antibody generated to the loop between TM8 and TM9 (see Annual Report 1994-1995 and ref.6). Therefore, it is likely that the glycosylation site in the loop between TM8 and TM9 was utilized in TM8-9R. This is consistent with model I topology, but not model III topology (Fig. 2). In support of this notion, the reporter molecule is approximately 31 kDa and thus would be too large to account for the 17-kDa membrane protected peptide. Based on the two models (I and II) that are consistent with our results, we conclude that TM9 displays stop-transfer activity, but only partially. It is noteworthy that a 36-kDa peptide was observed after proteinase K treatment and this peptide shifted to 34 kDa after PNGase F treatment (Fig. 3, lanes 3 and 4). Since TM8 can also insert in a  $N_{\text{exo}}-C_{\text{cyt}}$  orientation albeit to a much lesser extent (see Fig. 1B, lane 2), it is possible that TM9 reinitiated insertion into the membrane. Thus, treatment of membranes with proteinase K could result in a 36-kDa glycosylated peptide that corresponds to the amino acids containing TM9 and the reporter (Fig. 2, model III).

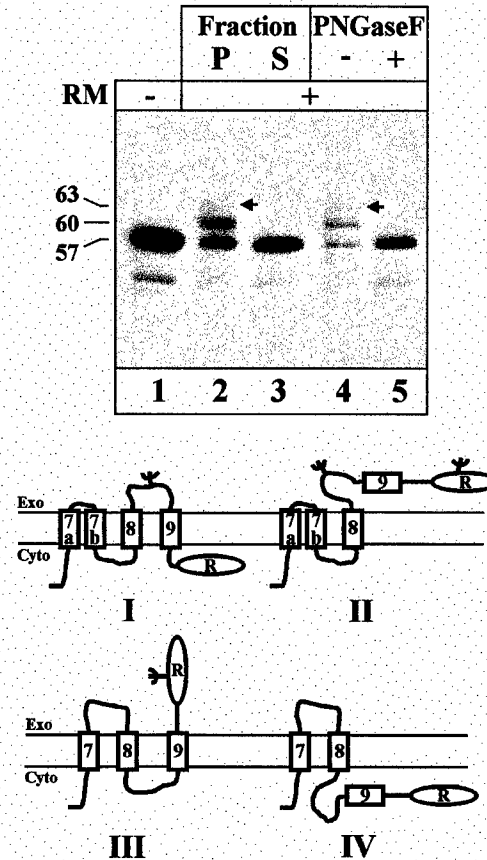
### *1.3. Membrane Topology of TM7-9R Construct.*

The above results indicate that the 17-kDa peptide generated after proteinase K treatment corresponds to a continuous stretch of amino acids spanning from TM8 to TM9. Since we used a construct that does not contain putative TM7, we were interested to see if TM8 and TM9 acted in the same manner in the presence of TM7. We created a DNA construct that codes for TM segments 7 through 9 followed by a glycosylation reporter (TM7-9R). Translation of TM7-9R transcript resulted in a 57-kDa product (Fig. 4, lane 1). In the presence of membranes, two additional bands of 60 and 63 kDa were observed and were clearly associated with membranes (Fig. 4, lanes 2 and 3). Treatment with PNGase F completely shifted the 60- and 63-kDa products to 57 kDa indicating that 1 and 2 N-linked sugars were attached to the 60- and 63-kDa products. We observed considerably less TM7-9R protein containing two sugars as compared with TM8-9R construct. This is likely to be a result of the membrane insertion properties of TM8 in the presence of TM7. We observed that TM8 favored a  $N_{\text{exo}}-C_{\text{cyt}}$  orientation in the presence of TM7 (see Fig. 1B, lane 5).

TM7-9R has three N-linked glycosylation consensus sites. In addition to the two sites mentioned already in TM8-9R, a site also exists just prior to putative TM7. To determine which sites were used, we treated membranes containing TM7-9R with proteinase K. Figure 3 (lane 5) shows three membrane-protected products of 45, 36, and 17 kDa, which were all glycosylated since PNGase F treatment resulted in the appropriate changes in gel mobility. These protected fragments were similar to those found for TM8-9R. This suggests that the membrane topologies for TM7-9R are likely the same as TM8-9R (compare Figs. 2 and 4, models I-III). In addition generation of these similar topologies was not disrupted by the presence of TM7. It is interesting to note that an

analysis. Taken together, these results suggest that TM9 has partial signal-anchor activity for membrane insertion.

**Figure 4. Translation of TM7-9R construct.** TM7-9R transcript was translated in the absence (lane 1) or presence of RM (lanes 2-5). Translation products were centrifuged to separate membrane (lane 2) and non-membrane fractions (lane 3). Membrane fractions were further treated with control solution (lane 4) or PNGase F (lane 5). Arrows denote a translation product that contains 2 N-linked sugars (see text). Models of TM7-9R topology are shown below. Symbols were described in Figure 2.

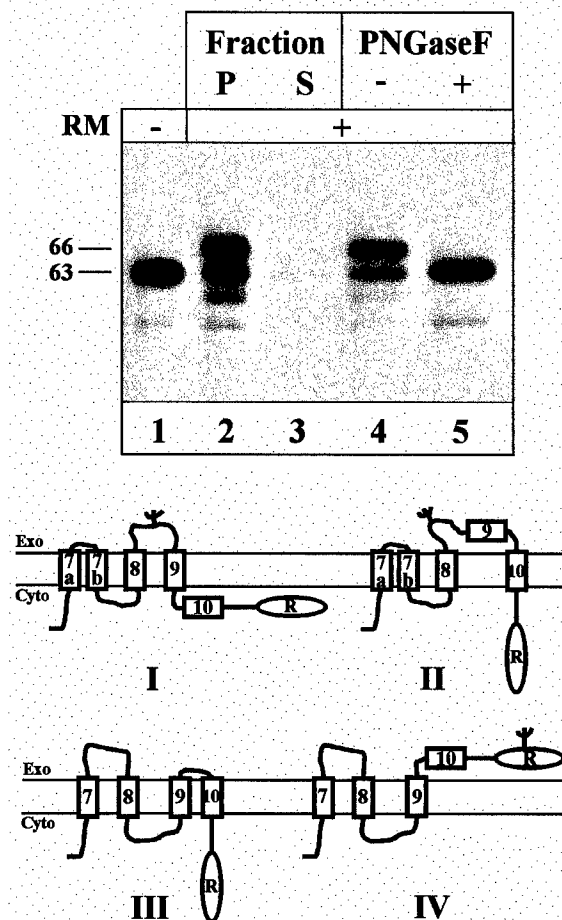


#### I.4. Membrane Topology of TM7-10R Construct.

Since we found that TM9 has partial stop-transfer activity, we were interested to know whether TM10 could act as a stop-transfer sequence when TM9 failed to anchor into membranes. To address this issue, we created a construct that contains TM7 through TM10 followed by a glycosylation reporter (TM7-10R). When translation of TM7-10R transcript was performed in the absence of membranes, a 63-kDa protein was generated (Fig. 5, lane 1). An additional 66-kDa product was produced in the presence of RM (Fig. 5, lane 2). Both products were found mostly in the pellet fraction after centrifugation indicating that the translation products were associated with membranes (Fig. 5, lanes 2 and 3). Treatment of membrane-associated products with the endoglycosidase PNGase F shifted the 66-kDa product (lane 4) to 63 kDa (lane 5). This indicates that the 66-kDa product was glycosylated and the change in molecular weight is consistent with the addition of a single high mannose core to the translation product. Since a translation product with 1 rather than 2 N-linked sugars was observed, this suggests that either TM9 functioned as a stop-transfer sequence while TM10 failed to reinitiate membrane insertion

(Fig. 5, model I) or TM10 functioned as a stop-transfer sequence (Fig. 5, model II). It is also possible that if TM9 reinitiated membrane insertion, TM10 may have failed to stop translocation across the membrane, resulting in a glycosylated reporter molecule (Fig. 5, model IV).

**Figure 5. Translation of TM7-10R.** TM7-10R transcript was translated in the absence (lane 1) or presence of RM (lanes 2-5). Translation products were centrifuged to separate membrane (lane 2) and non-membrane fractions (lane 3). Membrane fractions were further treated with control solution (lane 4) or PNGase F (lane 5). Models of TM7-10R topology are shown below. Symbols were described in Figure 2.



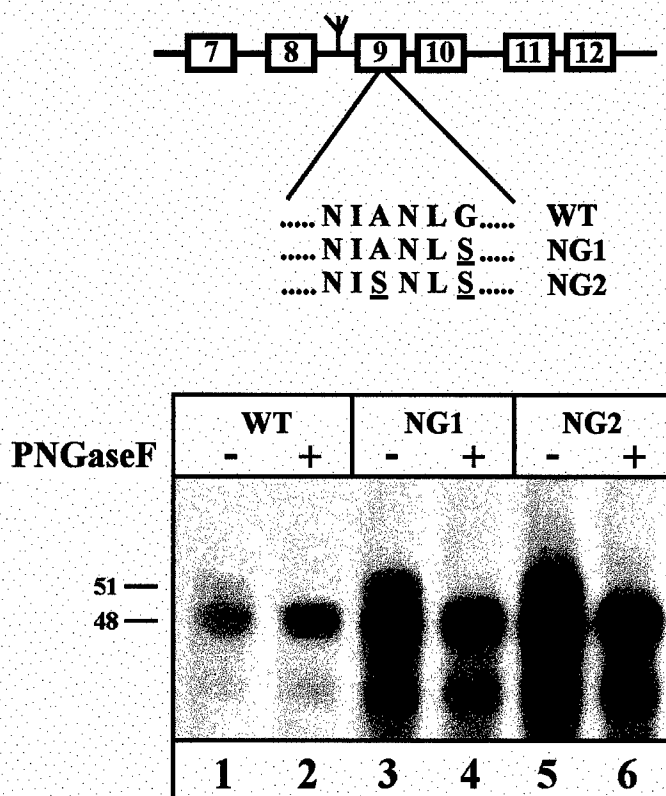
To test these models, proteinase K treatment of membranes was performed. Figure 3 (lane 7) reveals 39-kDa and 17-kDa peptide fragments that were resistant to proteinase K treatment. Both protected fragments were glycosylated since these bands shifted to 37 and 14 kDa, respectively, after PNGaseF treatment (Fig. 3, lane 8). The presence of a 17-kDa glycosylated peptide after proteinase K treatment indicates that TM9 functioned as a stop transfer sequence (Fig. 3, lanes 1 and 2). If TM9 failed to anchor into membranes while TM10 functioned as a stop-transfer sequence, a membrane-protected peptide that is 2-kDa larger would also be expected after proteinase K treatment. However, we failed to observe such a band. This suggests that TM9 completely anchored into membranes in the context of TM7-10R construct. The 39-kDa peptide fragment is consistent in molecular weight with peptide consisting of TM9 and TM10 and a glycosylated reporter molecule. This suggests that TM10 did not anchor into membranes. In addition, it should also be

noted that unglycosylated TM7-10R translation product was observed and would be consistent with model III (Fig. 5) topology where no consensus sites for glycosylation are exposed to the ER lumen. Taken together, our results indicate that TM9 has strong stop-transfer activity when TM10 is present. In addition, when TM9 acts as a signal-anchor sequence, TM10 displays only partial stop-transfer activity in the context of TM7-10R.

### 1.5. Accessibility of TM9 to the Lumen of the Endoplasmic Reticulum.

Based on our findings from TM7-9R and TM8-9R constructs, TM9 seems to display partial stop-transfer activity. However using TM7-10R construct, TM9 was able to completely stop the membrane translocation event and fully anchor in the membrane. This suggests that TM10 may facilitate the stop-transfer function of TM9. To examine the topological location of TM9 in a C-half Pgp molecule that contains the intact TM domain (i.e. TM domains 7-12), we assessed the accessibility of TM9 to the glycosylation machinery using a C-half Pgp which contains a consensus sequence for glycosylation within TM9. Using PCR mutagenesis technique, we replaced Gly<sup>841</sup> with Ser to generate

**Figure 6. Translation of C-half Pgp containing additional consensus sites for N-linked glycosylation.** One (NG-1) or two (NG-2) consensus sites for N-linked glycosylation were added within putative TM9 of the C-half Pgp construct, pGHaPGP-C6, by PCR site-directed mutagenesis. pGHaPGP-C6 encodes the C-half TM domain of Pgp. After translation, membrane-associated products were isolated by centrifugation and treated with control solution (lanes 1,3,5) or PNGase F (lanes 2,4,6). Note that only one N-linked sugar was observed for all constructs.



NG1 construct (Fig. 6). NG2 construct, which contains two N-linked glycosylation consensus sequences, contained an additional change where Ala<sup>838</sup> was replaced with a Ser residue. Translation of NG1 or NG2 transcript resulted in 51- and 49-kDa products (Fig. 6, lanes 3 and 5). The same bands were observed with the native C-half Pgp

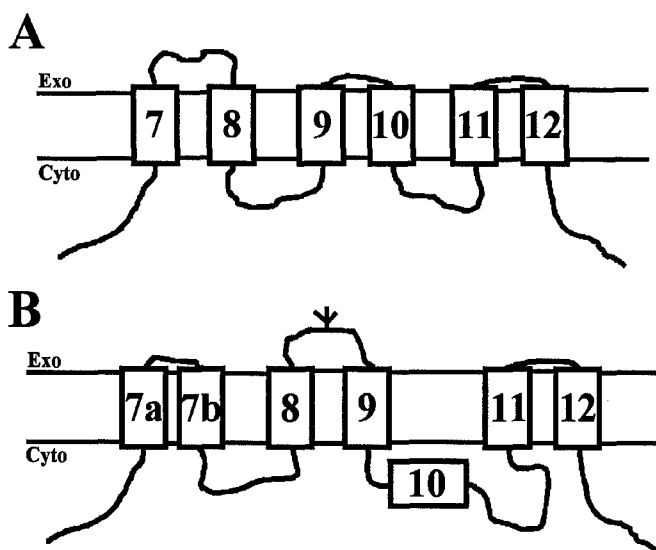
glycosylation within TM9. Using PCR mutagenesis technique, we replaced Gly<sup>841</sup> with Ser to generate NG1 construct (Fig. 6). NG2 construct, which contains two N-linked glycosylation consensus sequences, contained an additional change where Ala<sup>838</sup> was replaced with a Ser residue. Translation of NG1 or NG2 transcript resulted in 51- and 49-kDa products (Fig. 6, lanes 3 and 5). The same bands were observed with the native C-half Pgp sequence (Fig. 6, lane 1). For all three constructs, the 51-kDa product shifted to 49 kDa after PNGase F treatment, indicating the presence of one N-linked sugar. No additional glycosylation bands in NG1 and NG2 proteins were generated. Thus, TM9 in the C-half of Pgp is not exposed to the ER lumen.

### 1.6 Models for the Topology of Carboxyl-Terminal Half P-glycoprotein

The findings described indicate that the 17-kDa peptide resulting from protease treatment of membranes corresponds to a stretch of amino acids from TM8 to TM9. Importantly, this 17-kDa protease-resistant fragment had the same gel mobility as the protease-resistant fragment derived from the complete C-half transmembrane domain (see Annual Report 1994-1995 and (6). This finding is consistent with what has been previously observed in other studies which postulated alternate topologies for C-half Pgp. A glycosylated peptide derived from the C-half of Pgp with an approximate molecular size of 17-18 kDa was observed after protease digestion of membranes in topological studies involving mouse *mdr1* (8) and human *MDR3* Pgp (31). A 21-kDa glycosylated peptide was observed for human *MDR1* Pgp (9). This 21-kDa peptide is likely similar to our 17-kDa band and such a difference in molecular weight can be likely accounted for by differences in amino acid composition between species and/or variations in the estimation of molecular weight on SDS-PAGE. Taken together with previous findings, our results indicate that the alternate C-half topology can still maintain a six TM segment topology like the hydropathy model, but differs in that a "leave one out" topology is also adopted (Fig. 7).

**Figure 7. Model of C-half Pgp transmembrane domain.**

(A) Model based on hydropathy analysis of amino acid sequence and experimental results (Loo *et al.*, 1995; Kast *et al.*, 1996). (B) Topology of C-half Pgp based on experimental findings in this paper (TM9 and TM10) and others (for TM7 and TM8 see Beja *et al.*, 1995 and Han *et al.*, 1998; for TM11 and TM12 see Zhang *et al.*, 1993). Branched symbol represents N-linked glycosylation.



## **II. Functional analysis of Pgp**

Our previous results indicated that Pgp could be "locked" into a particular topology at least by introducing charged amino acids into the flanking regions of TM8 by site-directed mutagenesis (see Annual Report 1996-1997). By increasing the net positive charge flanking the C-terminal end of TM8, a greater fraction of Pgp molecules adopted the hydropathy-predicted model. In contrast, making the region flanking the C-terminal end of TM8 more negative in charge facilitated the generation of an alternative topology. Based on these observations, we were interested to ascertain any changes in Pgp function when cells expressed Pgp containing these charge mutations. Our goal was to examine both Pgp-mediated drug transport and regulation of endogenous swelling-activated chloride channels. In our last Annual Report (1996-1997), we introduced the charge mutations flanking TM8 into full-length Pgp cDNA and inserted these new constructs into a mammalian expression vector. Here, we describe the transfection, selection, and isolation of cells expressing either wild-type Pgp or Pgp containing the charge mutations described above (referred herein as mutant Pgp). Preliminary data on Pgp function are also described.

### *II.1. Transfection and Selection of Cells Expressing Mutant Pgp Constructs*

We decided to transfect our Pgp constructs into the mouse fibroblast cell line, BALB/c-3T3, since the transfection and selection procedures have been successfully used in our laboratory (see (19)). In general, we performed a liposome-mediated transfection and selected the transfected cell population with neomycin (G418). After propagation in G418, we isolated several colonies for each Pgp construct using cloning cylinders and propagated them. To screen rapidly for cells that express functional Pgp, we examined the ability of these colonies to transport the fluorescent Pgp substrate, rhodamine 123 (R123) (see METHODS, sec. V). Although it is possible that the presence of the introduced mutation can lead to a loss of Pgp function, we felt that this assay was a rapid method to screen for Pgp-expressing clones. A typical example that illustrates the transport of R123 in Pgp-expressing cells is shown in the figure below.

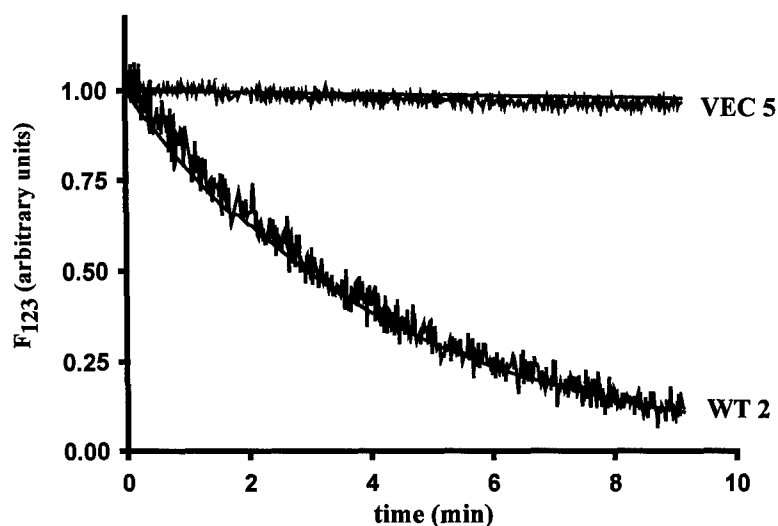


**Figure 8. Unidirectional efflux of the fluorescent Pgp-substrate, Rhodamine 123.** The decay in intracellular R123 fluorescence ( $F_{R123}$ ) was measured after superfusion with R123-free solution in BALB/c-3T3 cells transfected with vector (VEC 5) or wild-type Pgp (WT2). The decay in  $F_{R123}$  fits well to a single exponential (shown as a solid line superimposed on the  $F_{R123}$  trace). The R123 efflux is much larger in WT2 cells ( $k = 0.25 \text{ min}^{-1}$ ) as compared with VEC 5 cells ( $k = 0.003 \text{ min}^{-1}$ ).

Cells were loaded to steady-state with R123 (typically 1hr) and then were rapidly superfused with R123-free solution. The changes in intracellular fluorescence ( $F_{R123}$ ) were monitored on an inverted fluorescence microscope. In the absence of Pgp expression, relatively little change in  $F_{R123}$  was observed (Fig. 8, VEC 5). However, when Pgp was expressed in the plasma membrane, a rapid efflux of R123 was observed as a single exponential decay in  $F_{R123}$  (Fig. 8, WT2). It was also previously shown that the efflux of R123 is mediated by Pgp because the competitive inhibitor, verapamil, inhibited the decrease in  $F_{R123}$  (see ref.30).

When we screened cells that were transfected with mutant Pgp cDNA, we were able to identify colonies that likely expressed Pgp. However, for one construct, RRR (3 arginine residues added C-terminal to TM8), we failed to observe any substantial efflux of R123 in all isolated colonies examined. This could be due to the loss of proper biogenesis of Pgp (e.g., trapped in the endoplasmic reticulum) or failure to express Pgp. To test these possibilities, we performed western-blot analysis from isolated membranes of RRR constructs. We did not observe any substantial expression of Pgp in several RRR constructs tested (see Figure 9a for example). However, one RRR construct did reveal

Pgp expression, but the level was barely detectable by western-blot analysis. It is unclear why Pgp expression for RRR construct is very low to undetectable. In contrast, expression of Pgp was observed in many of the isolated colonies for all other mutant Pgp constructs. We selected several of these colonies for further characterization.

## II.2. Effect of Pgp Charge mutation on Transport of Rhodamine 123.

To examine the effect of Pgp mutations on Pgp drug transport function, we assessed both the expression of Pgp and the ability to transport R123 for the various Pgp mutants. Figures 9a and 9b show the estimated rate constant of R123 efflux for the various Pgp mutants tested, and western-blot analysis of Pgp expression from 150  $\mu$ g of isolated membranes is shown below. For wild-type Pgp, we observed that the relative expression of Pgp corresponded with the rate constant for R123 efflux (Fig. 9a). When we examined the mutant Pgps, there were some significant differences when comparing the relative expression with R123 efflux (Fig. 9b). E779D15 mutant seemed to have considerable R123 efflux, but relatively low expression when compared to wild-type Pgp, while K776E1 mutant had lower R123 efflux with relatively high expression.

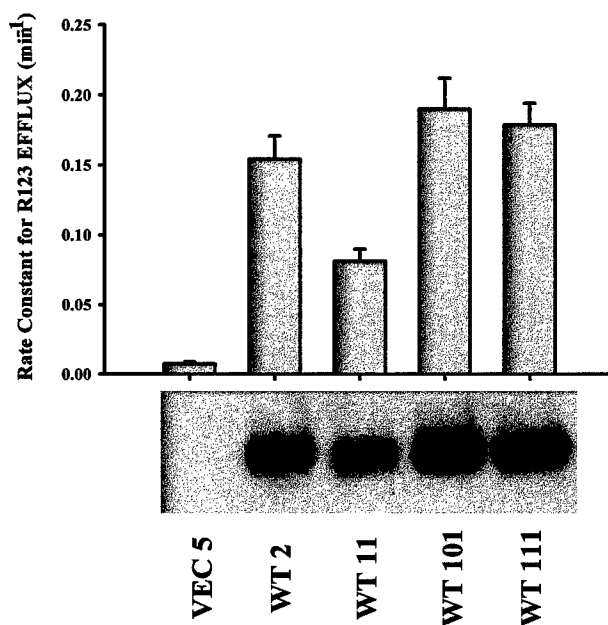


**Figure 9a. Expression of Pgp in isolated membranes from transfected cells and their estimated rate constants for efflux of rhodamine 123.** Expression of Pgp in isolated membranes (150  $\mu$ g) from vector- or wild-type Pgp- transfected cells was examined by Western blot analysis using anti-Pgp antibody, C494. Rate constants for R123 efflux for these transfected cells are shown directly above (see METHODS for determination of rate constants). Error bars are SEM (N= 4-5 experiments).



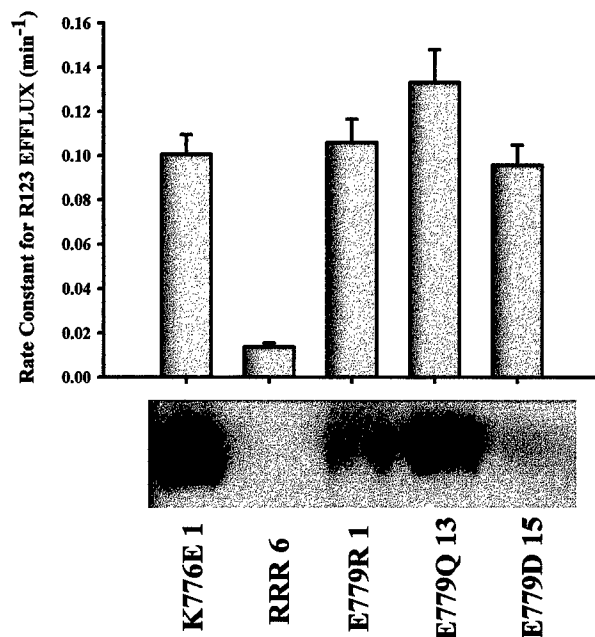
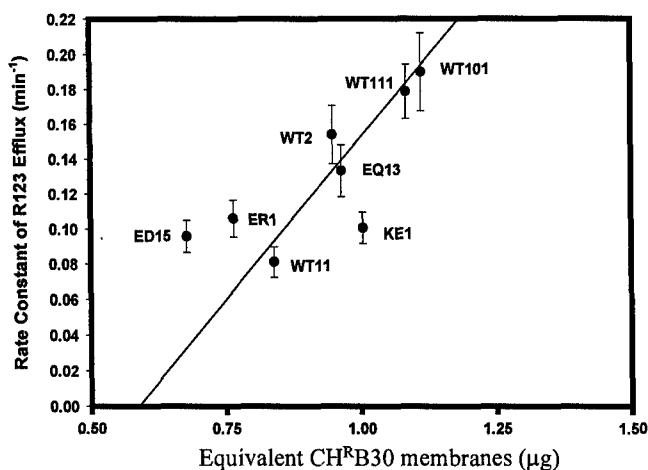


**Figure 9b. Expression of Pgp in isolated membranes from transfected cells and their estimated rate constants for efflux of rhodamine 123.** Same as Figure legend 9a except mutant Pgp-transfected cells are described.

For a more direct comparison between Pgp expression and R123 efflux, we performed quantitative western blot analysis using the monoclonal anti-Pgp antibody, C494. To ensure that the bands visualized on film were not saturated, we included membranes containing Pgp from Chinese hamster ovary cells (CH<sup>R</sup>B30) that were serially diluted. The signal detected from these control membranes was compared to the amount of control membranes analyzed. The signals derived from most wild-type and mutant Pgps fell within the linear range of detection for the control membranes (see below). Figure 10 shows the results from quantification of Pgp expression, which is plotted against the rate constant for R123 efflux. We have shown that K776E mutation facilitates generation of the alternate topology in a cell-free system. From Figure 10, we observed that the K776E1 mutant has less R123 transport than wild-type Pgp with similar Pgp expression levels (compare with WT 2). For E779D and E779Q mutants, we found relatively no effect on generation of Pgp topology, but E779R (and RRR) constructs favored the hydrophathy-predicted topology in the cell-free system (see Annual Report 1996-1997). From Figure 10, it seems that Pgp expression and R123 efflux do not follow any obvious trend consistent with the topological changes observed in the cell-free system. It should be noted, however, that the expression levels for E779D15 and E779R1 mutants were quite low. Furthermore, the western-blot signals did not lie within the linear range tested for control membranes. Therefore, quantitative assessments of expression for E779R1 and E779D mutants should be cautiously interpreted.

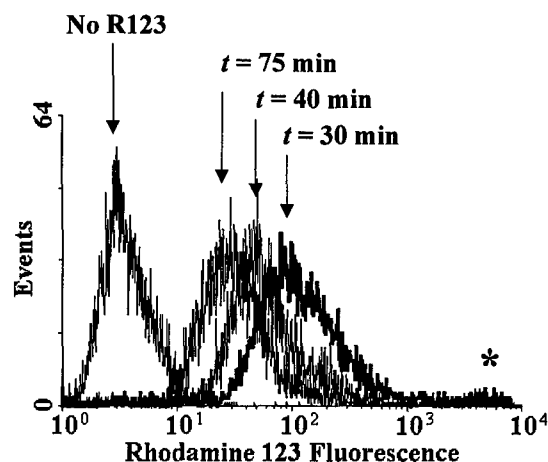
**Figure 10. Relationship between efflux of R123 and expression of Pgp.** Rate constants for R123 efflux was plotted as a function of Pgp expression, determined by quantitative western blot analysis. Pgp expression is represented as equivalent membranes isolated from the Pgp-expressing CH<sup>R</sup>B30 cells (see METHODS, sec.IV). The line represents the results from a linear regression analysis that was performed for all wild-type Pgps.



We are presently trying to use chemifluorescence technology in conjunction with a chemifluorescence detector (Molecular Dynamics Storm 860) as an alternative for quantitative analysis.

There are other considerations that need to be addressed. Since single colonies were isolated using a cloning cylinder, it is possible that a mixed population was obtained. For example, we could have obtained a mixed population of cells, with and without Pgp expression. This would result in an underestimation of both rate constants for R123 efflux and Pgp expression. To test this possibility, we examined the potential use of flow cytometry to assess the distribution of cells that express Pgp. The general idea was to first load a population of cells with R123 and then allow them to extrude R123. With enough time for R123 efflux, it may be possible to distinguish between populations that express different amounts of functional Pgp in the plasma membrane. Before we tested this idea, we wanted to determine whether any changes in

**Figure 11. Assessment of R123 efflux by flow cytometry.** To distinguish different population of cells, we loaded cells that were seeded in a T25 flask with 10 μM R123 to steady-state. Then, we allowed the cells that express functional Pgp (E779R1) to extrude R123 for varying amounts of time by replacing the external solution with R123-free solution. The cells were then isolated from the flask by exposure to trypsin and analyzed by a flow cytometer.



R123 fluorescence could be detected in cells using flow cytometry. We first loaded Pgp-expressing cells (E779R1) with 10  $\mu$ M R123 and then removed the extracellular solution with a R123-free solution to allow cells to lose R123 for different amounts of time. Cells were then recovered and analyzed by flow cytometry. Figure 11 shows that the level of intracellular R123 fluorescence decreases as the time allowed to lose R123 increases. This observation indicates that R123 is extruded from the cell with time and this change can be monitored by flow cytometry. Next, we examined other clones of Pgp using a similar assay. We allowed the cells to extrude R123 for over one hour and then examined the intracellular R123 fluorescence of cells by flow cytometry. Figure 12 shows that most of our isolated clones expressed a relatively homogeneous pattern of cells that extruded R123. However to our surprise, for both WT11 and E779D15, a significant subpopulation of cells was observed. Since a significant subpopulation appears to exist for WT11 and E779D15, we plan to sort these subpopulations and isolate only those cells that transport R123 by flow cytometry. Then, R123 transport and Pgp expression will be re-assessed in these clones.

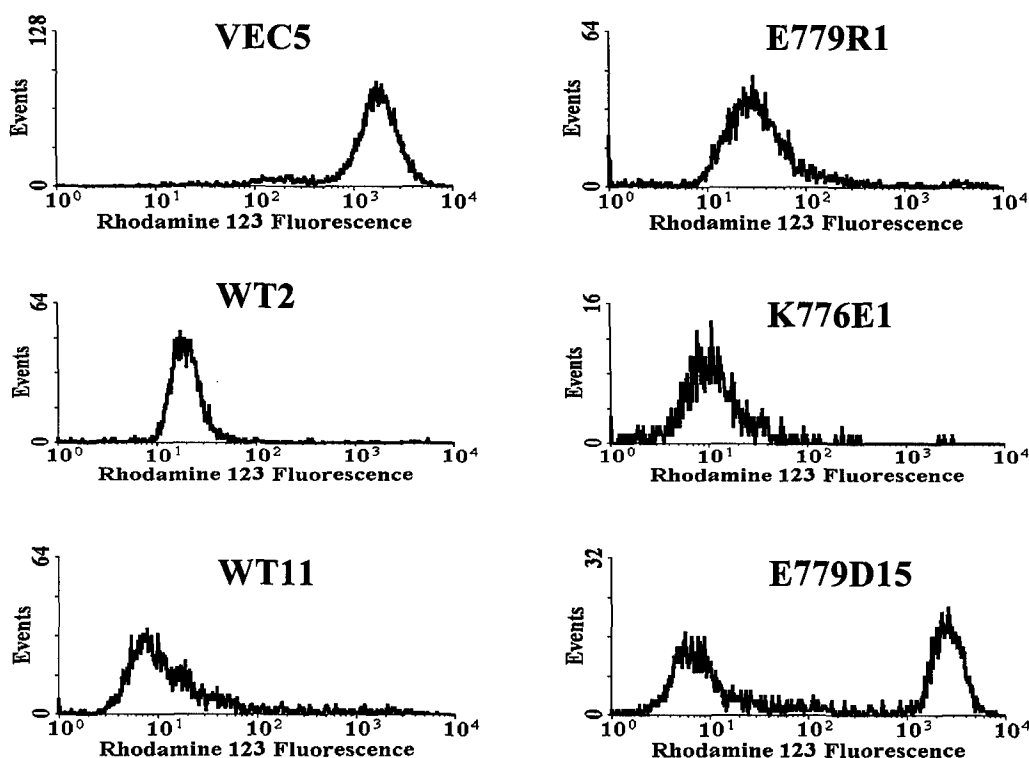


**Figure 12. Distribution of cells with intracellular rhodamine 123 fluorescence after 1hr incubation in R123-free solution.** Cells were loaded with 10  $\mu$ M R123 and then the extracellular solution was replaced with R123-free solution. After 1 hr, cells were recovered and intracellular R123 fluorescence was examined by flow cytometry.

## CONCLUSIONS

The main goal of this project has been to examine the structure and function of Pgp and to ascertain whether any relationship between the two exists. For determining Pgp structure, we focused on the C-terminal half of Pgp since little was known about its membrane folding. Although we initially planned to examine Pgp topology in breast cancer cells, we found that characterizing the C-half Pgp topology was facilitated using a cell-free system. In addition, the detailed mechanism of generating C-half Pgp topology could be directly assessed. Using this system, we found that the C-half of Pgp generates a topology different than predicted by the hydropathy model (Annual Report 1994-1995, 1995-1996 & 1996-1997).

In this report, we describe further studies of the topology of C-terminal half Pgp. We found that TM8 itself can insert into the membrane as a signal-anchor sequence in a  $N_{\text{cyt}}\text{-}C_{\text{exo}}$  orientation. We also observed that TM9 functions as a stop-transfer sequence to anchor into the membrane. This activity was dependent on the presence of TM10. Taken together, these data help define an alternative topological model for the C-half of Pgp. Interestingly, our model of the C-half of Pgp is different than predicted by the hydropathy model even though our model consists of 6 TM segments. Thus, the membrane insertion of the TM segments is much more complicated than predicted from the hydropathy model. Based on our cumulative studies of C-half Pgp topology, we hypothesize that the membrane insertion properties of TM8 play an important part in generating the multiple topological orientations for C-half Pgp. By inserting into membranes in a  $N_{\text{cyt}}\text{-}C_{\text{exo}}$  orientation, an alternative model can be generated. In addition, TM8 can also function as a stop-transfer sequence, which allows for the generation of the hydropathy-predicted model. Further studies are needed to confirm this alternative topology for C-half Pgp. The loop between TM8 and TM9 has already been observed to be extracellular in intact cells.

In order to examine how Pgp topology relates to function, we examined the possibility of "locking" Pgp into a particular topology. Then, we planned to assess the functions of the Pgp under this "locked" configuration. From our previous studies, we found that the anti-Pgp antibody C219 was able to block swelling-activated chloride currents in Pgp-expressing cells using the whole-cell patch-clamp technique (Annual Report 1994-1995). In addition, we performed an initial characterization of the channel(s) that are responsible for the swelling-activated chloride currents (Annual Report 1995-1996). Based on these results, we established a means to examine the channel-regulation function of Pgp. A technique to study the drug transport function of Pgp had already been established in our laboratory (see below).

In order to "lock" Pgp into a particular topology, we investigated the regulatory elements involved in generating multiple topological forms of Pgp. From our previous study examining regulatory elements of C-half Pgp, we found that the generation of C-half topologies could be manipulated by altering the charge distribution flanking TM8 (Annual Reports 1995-1996 & 1996-1997). Based on this observation, we were interested to know how Pgp functions were altered when these changes in charge distribution were studied in an intact cell. Here, we transfected cells with full-length Pgp cDNA that contains these charge changes flanking TM8. Pgp expression was observed for all

constructs transfected except for RRR construct. When we examined Pgp-mediated drug transport by assessing R123 efflux, we found that the K776E mutation decreased transport function relative to wild-type Pgp. It is currently unclear whether mutations that were created at glutamic acid residue 779 had any effect on drug transport. Interpretation of our data was confounded by the observation of a heterogeneous population from isolated colonies after transfection. We are now performing cell sorting by flow cytometry to isolate a homogenous population of cells for further studies. In addition, studies are currently in progress to examine the regulation of swelling-activated  $\text{Cl}^-$  currents by mutant Pgps. Since we have been able to express for the most part our mutant Pgp constructs in cells, functional analysis of these Pgp mutants will be possible. After all data are collected, we may be able to ascertain the effects of the Pgp mutants on Pgp functions and thus the relationship between Pgp structure and function.

## REFERENCES

1. Gottesman, M.M. and Pastan, I. (1993) *Annual Review of Biochemistry* **62**, 385-427
2. Higgins, C.F. (1993) *Current Opinion in Cell Biology* **5**, 684-687
3. Loo, T.W. and Clarke, D.M. (1995) *Journal of Biological Chemistry* **270**, 843-848
4. Kast, C., Canfield, V., Levenson, R., and Gros, P. (1995) *Biochemistry* **34**, 4402-4411
5. Kast, C., Canfield, V., Levenson, R., and Gros, P. (1996) *Journal of Biological Chemistry* **271**, 9240-9248
6. Han, E.S. and Zhang, J.-T. (1998) *Biochemistry*. In press.
7. Zhang, J.T., Duthie, M., and Ling, V. (1993) *Journal of Biological Chemistry* **268**, 15101-15110
8. Zhang, J.T. and Ling, V. (1991) *Journal of Biological Chemistry* **266**, 18224-18232
9. Skach, W.R., Calayag, M.C., and Lingappa, V.R. (1993) *Journal of Biological Chemistry* **268**, 6903-6908
10. Beja, O. and Bibi, E. (1996) *Proceedings of the National Academy of Sciences of the United States of America* **93**, 5969-5974
11. Beja, O. and Bibi, E. (1995) *Journal of Biological Chemistry* **270**, 12351-12354
12. Zhang, J.T. and Ling, V. (1993) *Biochimica et Biophysica Acta* **1153**, 191-202
13. Liao, S., Lin, J., Do, H., and Johnson, A.E. (1997) *Cell* **90**, 31-41
14. Wang, C., Chen, M., Han, E., and Zhang, J.T. (1997) *Biochemistry* **36**, 11437-11443
15. Seelig, A. (1998) *European Journal of Biochemistry* **251**, 252-261
16. Seelig, A. (1998) *International Journal of Clinical Pharmacology & Therapeutics* **36**, 50-54
17. Han, E.S., Vanoye, C.G., Altenberg, G.A., and Reuss, L. (1996) *American Journal of Physiology* **270**, C1370-C1378

18. Hardy, S.P., Valverde, M.A., Goodfellow, H.R., Higgins, C.F., and Sepulveda, F.V. (1994) *Japanese Journal of Physiology* **44 Suppl 2**, S9-15
19. Vanoye, C.G., Altenberg, G.A., and Reuss, L. (1997) *Journal of Physiology* **502**, 249-258
20. Gill, D.R., Hyde, S.C., Higgins, C.F., Valverde, M.A., Mintenig, G.M., and Sepulveda, F.V. (1992) *Cell* **71**, 23-32
21. Valverde, M.A., Diaz, M., Sepulveda, F.V., Gill, D.R., Hyde, S.C., and Higgins, C.F. (1992) *Nature* **355**, 830-833
22. McEwan, G.T., Hirst, B.H., and Simmons, N.L. (1994) *Biochimica et Biophysica Acta* **1220**, 241-247
23. Rasola, A., Galletta, L.J., Gruenert, D.C., and Romeo, G. (1994) *Journal of Biological Chemistry* **269**, 1432-1436
24. Morin, X.K., Bond, T.D., Loo, T.W., Clarke, D.M., and Bear, C.E. (1995) *Journal of Physiology* **486**, 707-714
25. Wu, J., Zhang, J.J., Koppel, H., and Jacob, T.J. (1996) *Journal of Physiology* **491**, 743-755
26. Higgins, C.F. (1995) *Cell* **82**, 693-696
27. Greger, R., Mall, M., Bleich, M., Ecke, D., Warth, R., Riedemann, N., and Kunzelmann, K. (1996) *Journal of Molecular Medicine* **74**, 527-534
28. Hartmann, E., Rapoport, T.A., and Lodish, H.F. (1989) *Proceedings of the National Academy of Sciences of the United States of America* **86**, 5786-5790
29. Devine, S.E., Ling, V., and Melera, P.W. (1992) *Proceedings of the National Academy of Sciences of the United States of America* **89**, 4564-4568
30. Altenberg, G.A., Vanoye, C.G., Horton, J.K., and Reuss, L. (1994) *Proceedings of the National Academy of Sciences of the United States of America* **91**, 4654-4657
31. Zhang, J.T. (1996) *Molecular Biology of the Cell* **7**, 1709-1721

## APPENDIX

### **I. Progress in the M.D.-Ph.D. program**

Currently, I am working towards completing the research requirements for my Ph.D. thesis in the Cellular Physiology and Molecular Biophysics Program, under the direction of both Drs. Jian-Ting Zhang (thesis advisor) and Luis Reuss (chairperson for thesis committee). I have been receiving continuous guidance and support from both of my mentors, who have been very helpful and encouraging. My projected completion of the requirements for a Ph.D. degree is November 1998.

### **II. Bibliography of Publications and Meeting Abstracts Supported by Predoctoral Fellowship DAMD17-94-4080**

#### **Publications:**

1. HAN,E., Vanoye,C.G., Altenberg, G.A., and Reuss,L. P-Glycoprotein-associated chloride currents revealed by specific block by an anti-P-glycoprotein antibody. Am.J.Physiol. 270 (Cell Physiol.39):C1370-C1378, 1996.
2. Wang, C., Chen, M., HAN, E., and Zhang, J.-T. Role of ribosomes in reinitiation of membrane insertion of integral transmembrane segments in a polytopic membrane protein. Biochem. 36 (38); 11437-11443, 1997.
3. Zhang, J.-T., Chen, M.A., HAN, E., and Wang, C.S. Dissection of *de novo* membrane insertion activities of internal transmembrane segments of ATP-binding-cassette transporters:toward understanding topological rules for membrane assembly of polytopic membrane proteins. Mol.Biol.Cell. 9: 853-863, 1998.
4. HAN, E. and Zhang, J.-T. Mechanism involved in generating the carboxyl-terminal half topology of P-glycoprotein. Biochem. In press.

#### **Abstracts:**

1. HAN,E., Vanoye-Trevino,C., Altenberg,G., and Reuss,L. Different properties of swelling-activated Cl<sup>-</sup> currents in P-Glycoprotein (Pgp) expressing and control cells. Biophys.J. 68(2):A273, 1995.
2. Reuss,L., Altenberg,G.A., Vanoye,C.G., and HAN,E.S. The P-glycoprotein of multidrug-resistant cells: solute pump and transporter regulator. J.Physiol.(Lond.) 489.P:12S-13S, 1995.
3. HAN,E., Chong, C.H., and Zhang, J.-T. Regulatory elements involved in the topogenesis of the C-terminal half of P-glycoprotein, a polytopic membrane protein.



Keystone Symposia: Protein Folding, Modification, and Transport in the Early Secretory Pathway, 1997.

4. HAN, E.S. and Zhang, J.-T. Mechanism of generating two membrane topologies for the C-terminal half P-glycoprotein. Proceedings of the American Association for Cancer Research. 39: 72, 1998.



## DEPARTMENT OF THE ARMY

US ARMY MEDICAL RESEARCH AND MATERIEL COMMAND  
504 SCOTT STREET  
FORT DETRICK, MARYLAND 21702-5012

REPLY TO  
ATTENTION OF:

MCMR-RMI-S (70-1y)

26 Jan 00

MEMORANDUM FOR Administrator, Defense Technical Information  
Center, ATTN: DTIC-OCA, 8725 John J. Kingman  
Road, Fort Belvoir, VA 22060-6218

SUBJECT: Request Change in Distribution Statement

1. The U.S. Army Medical Research and Materiel Command has  
reexamined the need for the limitation assigned to technical  
reports written for the following Awards.

DAMD17-86-C-6169	ADB116203
DAMD17-94-J-4056	ADB218947
DAMD17-94-J-4394	ADB220575
DAMD17-94-J-4358	ADB236080
DAMD17-94-J-4169	ADB236753
DAMD17-94-J-4049	ADB234453
DAMD17-94-J-4080	ADB218909
DAMD17-94-J-4080	ADB233428
DAMD17-94-J-4431	ADB220348
DAMD17-94-J-4335	ADB234557
DAMD17-94-J-4388	ADB218872
DAMD17-94-C-4081	ADB246577
DAMD17-94-J-4025	ADB238010
DAMD17-94-J-4080	ADB241898
MIPR 96MM6720	ADB240182
MIPR 96MM6720	ADB226818

Request the limited distribution statement for Accession Document  
Numbers be changed to "Approved for public release; distribution  
unlimited." These reports should be released to the National  
Technical Information Service.

2. Point of contact for this request is Ms. Virginia Miller at  
DSN 343-7327 or by email at virginia.miller@det.amedd.army.mil.

FOR THE COMMANDER:

PHYLLIS M. RINEHART  
Deputy Chief of Staff for  
Information Management